

Temperature Dependence of β -Ga₂O₃ Heteroepitaxy on c-plane Sapphire using Low Pressure Chemical Vapor Deposition

Gavax Joshi*, Yogesh Singh Chauhan, and Amit Verma#

Department of Electrical Engineering, Indian Institute of Technology Kanpur, India
Email: [*gajoshi@iitk.ac.in](mailto:gajoshi@iitk.ac.in), [#amitkver@iitk.ac.in](mailto:amitkver@iitk.ac.in)

Abstract. β -Ga₂O₃ has drawn significant attention for power electronics and deep ultraviolet (UV) photodetectors owing to its wide bandgap of ~ 4.4 - 4.9 eV and high electric breakdown strength ~7-8 MV/cm. Growth of β -Ga₂O₃ epitaxial thin films with high growth rate has been recently reported using low pressure chemical vapor deposition (LPCVD) technique. In this work, we have investigated the effect of growth temperature on β -Ga₂O₃ films grown on c-plane sapphire substrates using LPCVD. We performed growths by varying temperatures from 800 °C to 950 °C while keeping all other growth parameters (Ar/O₂ gas flow rates, growth pressure, and Gallium precursor to substrate distance) constant. Optical, structural, and surface characterizations are performed to determine the bandgap, phase purity, crystal orientation, and crystalline quality of the grown thin films. Amorphous islands of Ga₂O₃ are observed at growth temperature of 800 °C while continuous and crystalline (-201) oriented β -Ga₂O₃ thin films are achieved for growth temperatures of 850 °C to 950 °C. Crystallinity of the films is found to improve with increase in growth temperature with a minimum rocking full width at half maximum of 1.52° in sample grown at 925 °C. For all the samples grown at and above 875 °C, transmittance measurements revealed an optical bandgap of ~4.77-4.80 eV with high growth rate of ~6 μ m/hr.

Keywords: β -Ga₂O₃, low pressure chemical vapor deposition (LPCVD), wide bandgap, heteroepitaxy, thin film.

1. INTRODUCTION

Gallium Oxide (Ga₂O₃) crystallizes in five polymorphic forms: α , β , γ , δ , and ϵ [1]. Among these polymorphs, β -Ga₂O₃ is the most thermodynamically stable polymorph at room temperature [1]. β -Ga₂O₃ has a monoclinic crystal structure with a wide energy band gap of ~ 4.4 - 4.9 eV and high electrical breakdown (E_{br}) strength of ~ 7-8 MV/cm [2-4]. This theoretical estimation of E_{br} is ~3 times larger than other wide bandgap semiconductors such as GaN and SiC [5]. High E_{br} results in higher Baliga's and Johnson's figure of merit for β -Ga₂O₃ indicating its potential for highly efficient power devices with reduced conduction losses [6]. In the last few years, β -Ga₂O₃ Schottky barrier diodes with fast switching and high breakdown voltage [6-7], and β -Ga₂O₃ field-effect transistors (FETs) with lateral/vertical device structure [8-10], have been demonstrated with high power figure of merit and large breakdown voltage. Due to its wide bandgap, β -Ga₂O₃ has found applications as high performance solar-blind ultra-violet (UV)-photodetectors as well [11,12]. Properties of β -Ga₂O₃ are also suitable to realize gas sensors for harsh environment applications [13,14]. Because of its high laser damage threshold and high optical power tolerance, β -Ga₂O₃ is also a promising candidate for realizing dielectric laser accelerators and low loss plasmonics [15]. Besides its basic material advantages for various

applications, β -Ga₂O₃ also has an economical advantage over other wide-bandgap semiconductors because of the availability of high quality, large area single crystalline β -Ga₂O₃ substrates produced using low cost melt growth methods [16].

In order to realize various applications of β -Ga₂O₃, high quality epitaxial thin films of β -Ga₂O₃ with controlled doping are needed. Power electronics applications specially need thick vertical epilayers with low doping [17]. Epitaxial growth of β -Ga₂O₃ has been investigated using molecular beam epitaxy (MBE) [18-19], metal organic chemical vapor deposition (MOCVD) [20,21], mist-CVD [22], halide vapor phase epitaxy [23], pulse laser deposition [24], atomic layer deposition [25], and low pressure chemical vapor deposition (LPCVD) [26-29] among other techniques. LPCVD is an epitaxial growth method which has demonstrated fast β -Ga₂O₃ growth rates of up to 30 μ m/hr, under specific conditions, with controlled doping [30]. LPCVD is therefore quite promising for realization of high-power semiconductor devices with high breakdown voltage, as these devices need thick epilayers with low-doping concentrations.

The growth temperature plays a crucial role in deciding film quality during epitaxial growth as it provides surface migration energy to adatoms to reach the active growth sites [31]. Its role is even more important in β -Ga₂O₃ LPCVD as the growth temperature also decides the Ga flux. Thus, a detailed investigation of the material quality of β -Ga₂O₃ thin films as a function of growth temperature is required using LPCVD. In this work, on a customised in-house build LPCVD system, we have investigated the effect of varying the Ga source and substrate temperature on grown β -Ga₂O₃ thin films over c-plane sapphire (c-Al₂O₃) substrates while keeping the other growth parameters constant. The grown films have been characterized using optical, structural and surface characterization techniques to investigate the effect of growth temperature on material quality. The details of the experiment and characterizations are presented in the following sections.

2. EXPERIMENTAL DETAILS

For performing growths of β -Ga₂O₃ thin films, we used a customized single zone horizontal LPCVD reactor whose schematic is shown in Fig. 1(a). High purity Gallium metal (UMC, 99.99999% purity) and O₂ (99.9% purity) gas were used as source precursors and Argon (99.999% purity) was used as a carrier gas. The films were grown by keeping both the Ga source material and the c-plane Sapphire substrate in the center of a quartz tube (100 cm length and 2.7 cm inner diameter) with ~5 cm separation. The typical furnace temperature, Ar and O₂ flow rate profiles used for growth are shown in Fig. 1(b). The growth is started by pumping down the entire system to base pressure. After 5 minutes of pumping, Ar flow of 100 sccm is started which remains on during the rest of the growth and subsequent cool down. Furnace temperature is then ramped to reach the desired growth temperature with a ramp rate of ~4 °C /min. Once desired temperature is reached and stabilized, growth is started by flowing O₂ at a rate of 5 sccm. The tube pressure during the growth is maintained at ~ 100 Pa. After a growth period of 30 minutes, the oxygen flow is stopped, and the furnace is switched off and left to cool naturally under Ar flow. The deposited thin film was taken out at room temperature for further characterization. Before every growth, the c-plane Sapphire substrates were cleaned using acetone, isopropanol and de-ionized water for 10 minutes in ultrasonicator bath and dried with nitrogen flow. To study the effect of

growth temperature on the Ga₂O₃ thin film quality, six samples were grown with varying growth temperatures, T_g = 800 °C, 850 °C, 875 °C, 900 °C, 925 °C, and 950 °C.

The deposited β-Ga₂O₃ thin films were characterized for optical properties, thickness, surface morphology, phase purity, and crystal orientation. Cary 7000 Universal measurement spectrophotometer (Agilent technologies) was used to take transmission spectrum in UV and Visible range (200 nm – 800 nm). To extract the thickness of β-Ga₂O₃ thin films on sapphire, reflectance measurement was performed on Filmetrics, F20-EXR thin film analyzer. To obtain surface roughness of the samples, atomic force microscopy (AFM) was performed using Asylum research MFP-3D infinity system. To get surface topographical information, high resolution field emission scanning electron microscope (FESEM) imaging was done on Carl Zeiss Nova nanoSEM-450 and JEOL JSM-7100F, microscope. Raman spectroscopy was carried out on Princeton Instruments Acton Spectra Pro 2500i system with 532 nm solid state laser diode excitation. In-plane 2θ and rocking scans were performed on a PANalytical empyrean X-ray diffractometer with copper K_α radiation to determine film crystal orientation and quality. All the characterization measurements were done at room temperature.

3. RESULTS AND DISCUSSION

3.1 Optical Characterization

External optical transmission spectra as a function of wavelength (200 nm to 800 nm) of all the grown thin films are shown in Fig. 2(a). For thin films grown at T_g = 850 °C and above, absorption edge is observed in the UVC region around wavelength of 260 nm, suggesting growth of β- phase of Ga₂O₃. All the films show high optical transmission of ~60-80% in near UV and visible wavelength region. The transmittance increases with deposition temperature from ~65% at 850 °C to ~80% at 900 °C and then decreases to ~60% at 925 °C and 950 °C. The sharpness of the absorption edges also indicates crystalline nature of the β-Ga₂O₃ suggesting high quality thin films. The increase in transmittance is due to the improvement in crystallinity quality of β-Ga₂O₃ thin films with growth temperature and the decrease in the transmittance to ~60% at 925 °C and 950 °C, is possibly because of increase in O-vacancies in the films due to Ga-rich (O-poor) conditions at higher temperature which results in increase in absorption [32]. As β-Ga₂O₃ is close to a direct bandgap semiconductor [33], the power law dependence of absorption coefficient α is given by, $(\alpha h\nu)^2 \propto (h\nu - E_g)^{0.5}$, where $h\nu$ is the energy of the incident photon, and E_g is the band gap. Tauc plots to extract the optical bandgap of the grown thin films are shown in Fig. 2(b). We find extracted optical bandgap of ~4.77-4.88 eV which agrees well with the bandgap of β-Ga₂O₃ [2,3,33]. Optical bandgap dependence on T_g is shown in Fig. 2(c).

To measure the thickness of the films, we performed reflectance measurements. The thickness was extracted by modeling the reflectance data assuming reported values of β-Ga₂O₃ refractive index [34]. The extracted thickness as a function of T_g is shown in Fig. 2 (c). T_g = 850 °C sample was ~ 0.41 μm thick while all samples with T_g ≥ 875 °C had a thickness close to ~3 μm. The smaller thickness of T_g = 850 °C sample can be due to low Ga flux at this temperature. For all samples with T_g ≥ 875 °C, we found that the starting ~1 g Ga precursor was completely consumed by the end of the growth. This might be the reason for same thickness in all of these samples resulting from complete consumption of

the Ga precursor. The observed growth rate of $\sim 6 \mu\text{m/hr}$ for these samples is actually a lower bound on the real growth rate as the specific growth time when the Ga precursor is exhausted is not known. The actual growth rate is expected to be higher than $\sim 6 \mu\text{m/hr}$ for all samples with $T_g \geq 875 \text{ }^\circ\text{C}$. The observed growth rate is comparable to reported $\beta\text{-Ga}_2\text{O}_3$ growth rates using LPCVD [30].

The film grown at $T_g = 800 \text{ }^\circ\text{C}$ shows weak absorption for wavelengths less than $\sim 300 \text{ nm}$ with more than $\sim 60\%$ transparency at 200 nm . This observation suggests growth of defective Ga_2O_3 which has either incomplete coverage on c-plane (0001) sapphire substrate and/or its thickness is extremely thin allowing only partial absorption. To investigate on the substrate coverage of the film, we performed AFM of the sample. The AFM (Fig. 2(d)) shows small islands (height $\sim 0\text{-}100 \text{ nm}$) which do not coalesce to form a complete film. Similar observation can be made from Fig. 2(e) and Fig 2(f), showing surface FESEM image and EDS spectra of the sample grown at $T_g = 800 \text{ }^\circ\text{C}$. Small islands of width $\sim 50 - 70 \text{ nm}$ are clearly visible in FESEM. EDS composition analysis of surface shows O, Al and Ga atoms with atomic weight 53.39%, 44.02% and 2.59%, respectively. The presence of high concentration of Al confirms incomplete coverage of thin film over the entire substrate. The scattered and isolated islands of Ga_2O_3 are the reason for finite transmission even in deep UV for sample grown at $800 \text{ }^\circ\text{C}$. This morphology is possibly because of low Ga flux and low adatom energies at temperature of $800 \text{ }^\circ\text{C}$ which leads to island growth.

3.2 Raman Characterization

Fig. 3 shows measured Raman spectra of grown thin films excited using a 532 nm laser. Raman peak positions of the phonon modes, as observed in samples grown at different temperatures, are listed in table 1. Raman active modes are divided into three groups: high frequency ($\sim 770\text{-}500 \text{ cm}^{-1}$) due to stretching and bending of GaO_4 tetrahedra, mid frequency ($\sim 480 - 310 \text{ cm}^{-1}$) assigned to deformation of Ga_2O_6 and low frequency modes (below 200 cm^{-1}) are attributed to tetrahedra-octahedra chains [35]. As clear from Table 1, the obtained Raman modes are in good agreement with experimental and theoretical values reported in the literature [36]. No Raman peaks are obtained for Ga_2O_3 islands obtained at $T_g = 800 \text{ }^\circ\text{C}$ suggesting that the islands are amorphous. For sample grown at $850 \text{ }^\circ\text{C}$, only few Raman modes are activated suggesting that the thin film is of lower crystallinity as compared to other samples. For higher $T_g (\geq 875 \text{ }^\circ\text{C})$, all $\beta\text{-Ga}_2\text{O}_3$ phonon modes are observed in the measured Raman spectra which clearly indicates growth of phase pure $\beta\text{-Ga}_2\text{O}_3$ thin films.

3.3 XRD Characterization

XRD patterns of as-grown Ga_2O_3 thin films at different substrate temperatures are shown in Fig. 4. For $T_g = 800 \text{ }^\circ\text{C}$, no film diffraction peak is observed suggesting growth of amorphous Ga_2O_3 . This observation is consistent with the Raman measurements discussed in previous subsection. For thin films grown at $T_g \geq 850 \text{ }^\circ\text{C}$, three XRD diffraction peaks are observed at $\sim 18.9^\circ$, $\sim 38.3^\circ$ and $\sim 58.9^\circ$ respectively for all the samples. This indicates that the deposited Ga_2O_3 thin films are of (-201) orientation associated with the β -phase of Ga_2O_3 . The (-201) oriented family of planes is energetically more favorable over c-plane sapphire, because atomic configuration of the (-201) plane matches with that of c-plane sapphire [37]. For $T_g = 875 \text{ }^\circ\text{C}$, a small diffraction peak is also observed at 48.7° , which

corresponds to (510) peak of β -Ga₂O₃. This peak vanishes in samples grown at higher growth temperatures.

From the above discussion, we can conclude that all the samples with $T_g \geq 850$ °C show single phase (-201) oriented β -Ga₂O₃ thin films. However, the ratio of the intensity of (-201) and (-402) diffraction peaks ($I_{(-201)}/I_{(-402)}$) and the ratio of the intensity of (-603) and (-402) diffraction peaks ($I_{(-603)}/I_{(-402)}$) shows variation as T_g increases from 850 °C to 950 °C as shown in Fig. 5(a). Since there are no film diffraction peaks observed for sample grown at 800 °C, its intensity ratios are not shown in Fig. 5(a). The ideal values for these intensity ratios for β -Ga₂O₃ are also marked in the figure [38]. With increasing growth temperature, we observe that the measured XRD intensity ratios approach ideal values suggesting an improvement in the crystalline quality of the thin films. Similar conclusions can be drawn from Fig. 5(b), which shows decrease in full width half maximum (FWHM) of (-201), (-402) and (-603) diffraction peaks with increasing T_g . FWHM is calculated by fitting a gaussian function to each XRD peak. FWHM values decrease with increase in growth temperature, suggesting improvement in crystallinity of β -Ga₂O₃ thin films. Crystallite size is calculated using Scherrer (Eq. 1) [39] and Williamson-Hall (W-H) (Eq. 2) [39] formula where k is Scherrer's constant = 0.94, λ is wavelength of the X-ray radiation = 0.154060 nm, θ is the Bragg's angle, η is strain in the material, B_r is the FWHM of the diffraction peak, and D_S and D_{WH} are calculated crystallite size using Scherrer's and W-H method, respectively. Lower angle diffraction peak, (-201) reflection is considered for D_S calculation [39]. D_{WH} and strain is calculated from the intercept and the slope, respectively, by plotting $B_r \cos\theta$ vs $\sin\theta$ from Eq. 2 and fitting the data linearly.

$$D_S = \frac{k \lambda}{B_r \cos\theta} \quad \text{Eq. 1}$$

$$B_r \cos\theta = \frac{k \lambda}{D_{WH}} + \eta \sin\theta \quad \text{Eq. 2}$$

A plot comparing D_S and D_{WH} as a function of growth temperature is shown in Fig. 5(c). D_S increases from ~25 nm at $T_g = 850$ °C to ~27 nm for $T_g \geq 875$ °C. In comparison, D_{WH} is constant at ~28 nm and does not change with T_g ; the films are however found to be slightly strained with the strain decreasing with increasing growth temperature. This suggests that the β -Ga₂O₃ thin films deposited at higher temperature are much more relaxed. These results are consistent with previous β -Ga₂O₃ growth reports using different epitaxial methods [40-42].

Fig. 5(d) shows the XRD rocking scan of (-402) family of planes for β -Ga₂O₃ films grown at 850 °C and above. The rocking FWHM values of the films grown at 850 °C, 875 °C, 900 °C, 925 °C and 950 °C are 1.61°, 2.12°, 1.91°, 1.5°, and 1.64°, respectively, as shown in Fig. 5(e). Among the samples of similar thickness ($T_g = 875$ °C - 950 °C), the rocking FWHM value is highest for β -Ga₂O₃ film grown at 875 °C and lowest for film grown at 925 °C. This decrease in FWHM value of the diffraction peak suggests improvement in the crystal quality with growth temperature till $T_g = 925$ °C. To explore the nature of epitaxial relationship between β -Ga₂O₃ thin film and c-plane sapphire substrate, we performed off-axis ϕ scan for diffraction plane (111) for $T_g = 925$ °C sample (Fig. 5(f)). In-plane 6-fold rotational symmetry is visible from presence of six peaks separated by 60°. Since, β -Ga₂O₃ has a 2-fold in-plane symmetry which is grown on a c-plane sapphire substrate with 3-fold rotational symmetry, the presence of 6 peaks in the ϕ scan suggests presence of rotational domains in the thin film [43].

3.4 Surface Characterization

Fig. 6 shows top surface AFM scan for the scan area of $5\ \mu\text{m} \times 5\ \mu\text{m}$ for samples deposited at different temperatures. The dependence of surface morphology, and crystallinity on the growth temperature is clearly visible in images. $\beta\text{-Ga}_2\text{O}_3$ islands formed at $800\ \text{°C}$ (Fig. 2(d)) gets coalesced into a continuous thin film at higher growth temperature. As deposition temperature is increased ($\geq 850\ \text{°C}$) the crystallinity is improved and change in surface morphology is also observed. As shown in Fig. 6 graph, variation in mean RMS roughness is seen as growth temperature is increased from $850\ \text{°C}$ to $900\ \text{°C}$ and stays almost constant for higher growth temperatures. The smoothest thin films are obtained at $T_g = 850\ \text{°C}$, which is also confirmed by interference fringes in transmittance spectra as shown in Fig. 2(a).

To analyse the top surface morphology and elemental composition, FESEM and EDS was performed. Top view FESEM image of $T_g = 950\ \text{°C}$ sample is shown in Fig. 7(a). Hexagonal crystal edges at the surface are clearly visible which matches with the 6-fold symmetry of the substrate and the $(-201)\ \beta\text{-Ga}_2\text{O}_3$. EDS spectra of the sample was done to determine the chemical composition. EDS spectra result is shown in Fig. 7(b). The atomic weight percentage of Ga and O was found to be $\sim 77.9\%$ and $\sim 22.1\%$, respectively, suggesting that the grown films have the correct stoichiometric composition.

4. CONCLUSIONS

$\beta\text{-Ga}_2\text{O}_3$ thin films were synthesized on c-plane sapphire substrate using LPCVD. The effect of varying the growth temperature (from $800\ \text{°C}$ to $950\ \text{°C}$) on the optical and the structural properties of the $\beta\text{-Ga}_2\text{O}_3$ films was studied. Amorphous Ga_2O_3 islands were obtained for the growth temperature of $800\ \text{°C}$, while continuous and crystalline $(-201)\ \beta\text{-Ga}_2\text{O}_3$ films were obtained for the growth temperature of $850\ \text{°C}$ - $950\ \text{°C}$. Films grow with a high growth rate of $\sim 6\ \mu\text{m/hr}$ for T_g of $875\ \text{°C}$ - $950\ \text{°C}$. Crystallinity of the films was found to significantly improve with the increase in growth temperature with the best quality films obtained for $T_g = 900\ \text{°C}$ - $950\ \text{°C}$. LPCVD growth of $\beta\text{-Ga}_2\text{O}_3$ thin films with good crystalline quality at high growth rates will help enable the applications of this material in high power transistors, deep UV photodetectors, and harsh environment sensors.

ACKNOWLEDGEMENT

This work was supported by SERB Early Career Research Award (Grant No. ECR/2018/001076) and used XRD (supported by DST-FIST Grant No. SR/FST/ETII-053/2012) and Raman characterization facilities of Dept. of Materials Science and Engineering, IIT Kanpur. Authors also thank A. Kalra and Dr. D. Nath from Indian Institute of Science, Bangalore for help with few XRD measurements.

REFERENCES

- [1] Roy, Rustum, V. G. Hill, and E. F. Osborn. "Polymorphism of Ga₂O₃ and the system Ga₂O₃—H₂O." *Journal of the American Chemical Society* 74, no. 3 (1952): 719-722.
- [2] Tippins, H. H. "Optical absorption and photoconductivity in the band edge of β-Ga₂O₃." *Physical Review* 140, no. 1A (1965): A316.
- [3] Onuma, Takeyoshi, Shingo Saito, Kohei Sasaki, Tatekazu Masui, Tomohiro Yamaguchi, Tohru Honda, and Masataka Higashiwaki. "Valence band ordering in β-Ga₂O₃ studied by polarized transmittance and reflectance spectroscopy." *Japanese Journal of Applied Physics* 54, no. 11 (2015): 112601.
- [4] Higashiwaki, Masataka, Kohei Sasaki, Akito Kuramata, Takekazu Masui, and Shigenobu Yamakoshi. "Gallium oxide (Ga₂O₃) metal-semiconductor field-effect transistors on single-crystal β-Ga₂O₃ (010) substrates." *Applied Physics Letters* 100, no. 1 (2012): 013504. <https://doi.org/10.1063/1.3674287>
- [5] Pearton, S. J., Jiancheng Yang, Patrick H. Cary IV, F. Ren, Jihyun Kim, Marko J. Tadjer, and Michael A. Mastro. "A review of Ga₂O₃ materials, processing, and devices." *Applied Physics Reviews* 5, no. 1 (2018): 011301. <https://doi.org/10.1063/1.5006941>
- [6] Li, Wenshen, Zongyang Hu, Kazuki Nomoto, Riena Jinno, Zexuan Zhang, Thieu Quang Tu, Kohei Sasaki, Akito Kuramata, Debdeep Jena, and Huili Grace Xing. "2.44 kV Ga₂O₃ vertical trench Schottky barrier diodes with very low reverse leakage current." In *2018 IEEE International Electron Devices Meeting (IEDM)*, pp. 8-5. IEEE, 2018. doi: 10.1109/IEDM.2018.8614693
- [7] Yang, Jiancheng, Fan Ren, Marko Tadjer, S. J. Pearton, and A. Kuramata. "2300V reverse breakdown voltage Ga₂O₃ schottky rectifiers." *ECS Journal of Solid State Science and Technology* 7, no. 5 (2018): Q92. <https://doi.org/10.1149/2.0241805jss>
- [8] Tetzner, Kornelius, Eldad Bahat Treidel, Oliver Hilt, Andreas Popp, Saud Bin Anooz, Günter Wagner, Andreas Thies, Karina Ickert, Hassan Gargouri, and Joachim Würfl. "Lateral 1.8 kV β-Ga₂O₃ MOSFET with 155 MW/cm² Power Figure of Merit." *IEEE Electron Device Letters* 40, no. 9 (2019): 1503-1506. doi: 10.1109/LED.2019.2930189
- [9] Li, W., K. Nomoto, Z. Hu, T. Nakamura, D. Jena, and H. G. Xing. "Single and multi-fin normally-off Ga₂O₃ vertical transistors with a breakdown voltage over 2.6 kV." In *2019 IEEE International Electron Devices Meeting (IEDM)*, pp. 12-4. IEEE, 2019. <https://doi.org/10.1109/IEDM19573.2019.8993526>
- [10] Zhang, Hongpeng, Lei Yuan, Xiaoyan Tang, Jichao Hu, Jianwu Sun, Yimen Zhang, Yuming Zhang, and Renxu Jia. "Progress of Ultra-Wide Bandgap Ga₂O₃ Semiconductor Materials in Power MOSFETs." *IEEE Transactions on Power Electronics* 35, no. 5 (2019): 5157-5179. <https://doi.org/10.1109/TPEL.2019.2946367>
- [11] Li, Shan, Daoyou Guo, Peigang Li, Xia Wang, Yuehui Wang, Zuyong Yan, Zeng Liu et al. "Ultrasensitive, Superhigh Signal-to-Noise Ratio, Self-Powered Solar-Blind Photodetector Based on n-Ga₂O₃/p-CuSCN Core–Shell Microwire Heterojunction."

- ACS applied materials & interfaces 11, no. 38 (2019): 35105-35114.
<https://doi.org/10.1021/acsami.9b11012>
- [12] Li, Shan, Zuyong Yan, Zeng Liu, Jun Chen, Yusong Zhi, Daoyou Guo, Peigang Li, Zhenping Wu, and Weihua Tang. "A self-powered solar-blind photodetector with large V_{oc} enhancing performance based on the PEDOT: PSS/Ga₂O₃ organic–inorganic hybrid heterojunction." *Journal of Materials Chemistry C* 8, no. 4 (2020): 1292-1300.
<https://doi.org/10.1039/C9TC06011A>
- [13] Baban, C., Y. Toyoda, and M. Ogita. "Oxygen sensing at high temperatures using Ga₂O₃ films." *Thin Solid Films* 484, no. 1-2 (2005): 369-373.
<https://doi.org/10.1016/j.tsf.2005.03.001>
- [14] Lampe, U., M. Fleischer, and H. Meixner. "Lambda measurement with Ga₂O₃." *Sensors and Actuators B: Chemical* 17, no. 3 (1994): 187-196.
[https://doi.org/10.1016/0925-4005\(93\)00880-8](https://doi.org/10.1016/0925-4005(93)00880-8)
- [15] Deng, Huiyang, Kenneth J. Leedle, Yu Miao, Dylan S. Black, Karel E. Urbanek, Joshua McNeur, Martin Kozák et al. "Gallium Oxide for High-Power Optical Applications." *Advanced Optical Materials* 8, no. 7 (2020): 1901522.
<https://doi.org/10.1002/adom.201901522>
- [16] Mohamed, H. F., Changtai Xia, Qinglin Sai, Huiyuan Cui, Mingyan Pan, and Hongji Qi. "Growth and fundamentals of bulk β -Ga₂O₃ single crystals." *Journal of Semiconductors* 40, no. 1 (2019): 011801
<https://doi.org/10.1088/1674-4926/40/1/011801>
- [17] Baldini, Michele, Zbigniew Galazka, and Günter Wagner. "Recent progress in the growth of β -Ga₂O₃ for power electronics applications." *Materials Science in Semiconductor Processing* 78 (2018): 132-146.
<https://doi.org/10.1016/j.mssp.2017.10.040>.
- [18] Singh Pratiyush, Anamika, Sriram Krishnamoorthy, Swanand Vishnu Solanke, Zhanbo Xia, Rangarajan Muralidharan, Siddharth Rajan, and Digbijoy N. Nath. "High responsivity in molecular beam epitaxy grown β -Ga₂O₃ metal semiconductor metal solar blind deep-UV photodetector." *Applied Physics Letters* 110, no. 22 (2017): 221107. <https://doi.org/10.1063/1.4984904>
- [19] Okumura, Hironori, Masao Kita, Kohei Sasaki, Akito Kuramata, Masataka Higashiwaki, and James S. Speck. "Systematic investigation of the growth rate of β -Ga₂O₃ (010) by plasma-assisted molecular beam epitaxy." *Applied Physics Express* 7, no. 9 (2014): 095501. <https://doi.org/10.7567/APEX.7.095501>
- [20] Feng, Zixuan, A. F. M. Anhar Uddin Bhuiyan, Md Rezaul Karim, and Hongping Zhao. "MOCVD homoepitaxy of Si-doped (010) β -Ga₂O₃ thin films with superior transport properties." *Applied Physics Letters* 114, no. 25 (2019): 250601.
<https://doi.org/10.1063/1.5109678>
- [21] Ghadi, Hemant, Joe F. McGlone, Christine M. Jackson, Esmat Farzana, Zixuan Feng, AFM Anhar Uddin Bhuiyan, Hongping Zhao, Aaron R. Arehart, and Steven A. Ringel. "Full bandgap defect state characterization of β -Ga₂O₃ grown by metal

- organic chemical vapor deposition." *APL Materials* 8, no. 2 (2020): 021111.
<https://doi.org/10.1063/1.5142313>
- [22] Xu, Yu, Zhiyuan An, Lixin Zhang, Qian Feng, Jincheng Zhang, Chunfu Zhang, and Yue Hao. "Solar blind deep ultraviolet β -Ga₂O₃ photodetectors grown on sapphire by the Mist-CVD method." *Optical Materials Express* 8, no. 9 (2018): 2941-2947.
<https://doi.org/10.1364/OME.8.002941>
- [23] Leach, J. H., K. Uduary, J. Rumsey, G. Dodson, H. Splawn, and K. R. Evans. "Halide vapor phase epitaxial growth of β -Ga₂O₃ and α -Ga₂O₃ films." *APL Materials* 7, no. 2 (2019): 022504. <https://doi.org/10.1063/1.5055680>
- [24] Q. Guo, K. Nishihagi, Z. Chen, K. Saito, T. Tanaka, Characteristics of thulium doped gallium oxide films grown by pulsed laser deposition, *Thin Solid Films*. 639 (2017) 123–126. <https://doi.org/10.1016/j.tsf.2017.08.038>
- [25] D. Choi, K.-B. Chung, J.-S. Park, Low temperature Ga₂O₃ atomic layer deposition using gallium tri-isopropoxide and water, *Thin Solid Films*. 546 (2013) 31–34.
<https://doi.org/10.1016/j.tsf.2013.03.066>
- [26] S. Rafique, L. Han, H. Zhao, Synthesis of wide bandgap Ga₂O₃ ($E_g \sim 4.6$ - 4.7 eV) thin films on sapphire by low pressure chemical vapor deposition, *Phys. Status Solidi Appl. Mater. Sci.* 213 (2016) 1002–1009. <https://doi.org/10.1002/pssa.201532711>
- [27] S. Rafique, L. Han, C.A. Zorman, H. Zhao, Synthesis of Wide Bandgap β -Ga₂O₃ Rods on 3C-SiC-on-Si, *Cryst. Growth Des.* 16 (2016) 511–517.
<https://doi.org/10.1021/acs.cgd.5b01562>
- [28] S. Rafique, L. Han, A.T. Neal, S. Mou, M.J. Tadjer, R.H. French, H. Zhao, Heteroepitaxy of N-type β -Ga₂O₃ thin films on sapphire substrate by low pressure chemical vapor deposition, *Appl. Phys. Lett.* 109 (2016) 0–5.
<https://doi.org/10.1063/1.4963820>
- [29] Zhang, Yuxuan, Zixuan Feng, Md Rezaul Karim, and Hongping Zhao. "High-temperature low-pressure chemical vapor deposition of β -Ga₂O₃." *Journal of Vacuum Science & Technology A: Vacuum, Surfaces, and Films* 38, no. 5 (2020): 050806.
<https://doi.org/10.1116/6.0000360>
- [30] Z. Feng, M.R. Karim, H. Zhao, Low pressure chemical vapor deposition of β -Ga₂O₃ thin films: Dependence on growth parameters, *APL Mater.* 7 (2019) 022514.
<https://doi.org/10.1063/1.5054713>
- [31] S. Rafique, L. Han, S. Mou, H. Zhao, Temperature and doping concentration dependence of the energy band gap in β -Ga₂O₃ thin films grown on sapphire, *Opt. Mater. Express*. 7 (2017) 3561. <https://doi.org/10.1364/ome.7.003561>
- [32] Dong, Linpeng, Renxu Jia, Bin Xin, Bo Peng, and Yuming Zhang. "Effects of oxygen vacancies on the structural and optical properties of β -Ga₂O₃." *Scientific reports* 7, no. 1 (2017): 1-12. <https://doi.org/10.1038/srep40160>

- [33] M. Mohamed, C. Janowitz, I. Unger, R. Manzke, Z. Galazka, R. Uecker, R. Fornari, J.R. Weber, J.B. Varley, C.G. Van De Walle, The electronic structure of β -Ga₂O₃, *Appl. Phys. Lett.* 97 (2010) 2–5. <https://doi.org/10.1063/1.3521255>
- [34] M. Rebien, W. Henrion, M. Hong, J.P. Mannaerts, M. Fleischer, Optical properties of gallium oxide thin films, *Appl. Phys. Lett.* 81 (2002) 250–252. <https://doi.org/10.1063/1.1491613>
- [35] D. Dohy, G. Lucazeau, A. Revcolevschi, Raman spectra and valence force field of single-crystalline β Ga₂O₃, *J. Solid State Chem.* 45 (1982) 180–192. [https://doi.org/10.1016/0022-4596\(82\)90274-2](https://doi.org/10.1016/0022-4596(82)90274-2)
- [36] C. Kranert, C. Sturm, R. Schmidt-grund, M. Grundmann, Raman tensor elements of β -Ga₂O₃, *Nat. Publ. Gr.* (2016) 1–9. <https://doi.org/10.1038/srep35964>
- [37] W. Seiler, M. Selmane, K. Abdelouhadi, J. Perrière, Epitaxial growth of gallium oxide films on c-cut sapphire substrate, *Thin Solid Films.* 589 (2015) 556–562. <https://doi.org/10.1016/j.tsf.2015.06.034>
- [38] K. Momma, F. Izumi, VESTA 3 for three-dimensional visualization of crystal, volumetric and morphology data, *J. Appl. Crystallogr.* 44 (2011) 1272–1276. <https://doi.org/10.1107/S0021889811038970>
- [39] C. Suryanarayana, M.G. Norton, *X-Ray Diffraction: A Practical Approach*, 1st ed., Springer US, 1998. <https://doi.org/10.1007/978-1-4899-0148-4>
- [40] G.A. Battiston, R. Gerbasi, M. Porchia, R. Bertocello, F. Caccavale, Chemical vapour deposition and characterization of gallium oxide thin films, *Thin Solid Films.* 279 (1996) 115–118. [https://doi.org/10.1016/0040-6090\(95\)08161-5](https://doi.org/10.1016/0040-6090(95)08161-5)
- [41] Q. Feng, F. Li, B. Dai, Z. Jia, W. Xie, T. Xu, X. Lu, X. Tao, J. Zhang, Y. Hao, The properties of gallium oxide thin film grown by pulsed laser deposition, *Appl. Surf. Sci.* 359 (2015) 847–852. <https://doi.org/10.1016/j.apsusc.2015.10.177>
- [42] K. Yoshihiro, M. Kasumi, E. Fumie, N. Shinji, Sol-gel prepared thin films for ultraviolet photodetectors, *Appl. Phys. Lett.* 90. 031912 (2007) 1–4. <https://doi.org/10.1063/1.2432946>
- [43] T. Oshima, T. Okuno, F. Shizuo, Ga₂O₃ Thin Film Growth on c-Plane Sapphire Substrates by Molecular Beam Epitaxy for Deep- Ultraviolet Photodetectors, *Jpn. J. Appl. Phys.* 46 (2007) 7217–7220. <https://doi.org/10.1143/JJAP.46.7217>

Table 1: Measured Raman peak spectral positions of the phonon modes in LPCVD grown β -Ga₂O₃ thin films

(n.o = not observed).

Raman phonon modes	Growth Temperature					Experimental Reference [36]	Theoretical Reference [36]
	850 °C	875 °C	900 °C	925 °C	950 °C		
B_g^2	143.3	146.6	146.6	146.6	145.2	144.8	145.6
A_g^2	168.9	169.5	169.4	170.8	170.8	169.9	176.4
A_g^3	199.7	200.3	200.3	200.3	200.3	200.2	199.1
A_g^4	n.o.	319.8	319.8	319.8	321.1	320.0	318.5
A_g^5	348.2	347.4	347.4	348.7	347.4	346.6	342.5
A_g^6	416.2	416.8	416.8	416.8	416.8	416.2	432
A_g^7	n.o.	475.2	476.4	475.2	479	474.9	472.8
A_g^8	n.o.	631.4	632.6	633.9	631.4	630.0	624.4
B_g^5	657.4	652.9	652.9	655.4	652.9	652.3	653.9
A_g^{10}	770.3	767.1	768.4	769.6	767.1	766.7	767.0

List of Figures

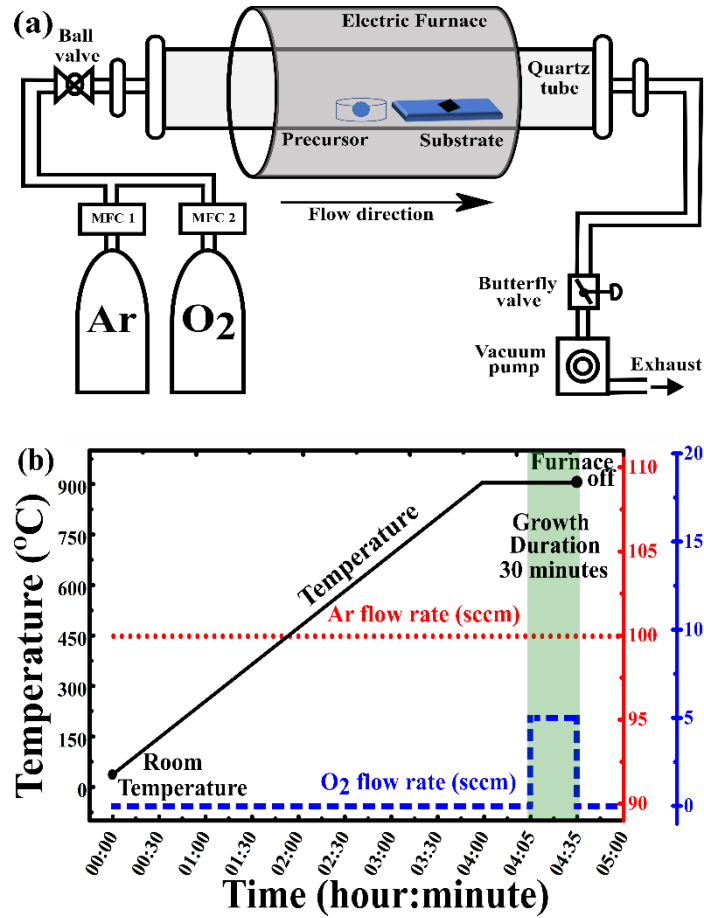


Figure 1: (a) Schematic of the LPCVD reactor setup used for the synthesis of β -Ga₂O₃ thin films, and (b) Temperature (for $T_g = 900$ °C), Argon gas flow rate, and O₂ gas flow rate profiles for LPCVD growth of β -Ga₂O₃ thin film.

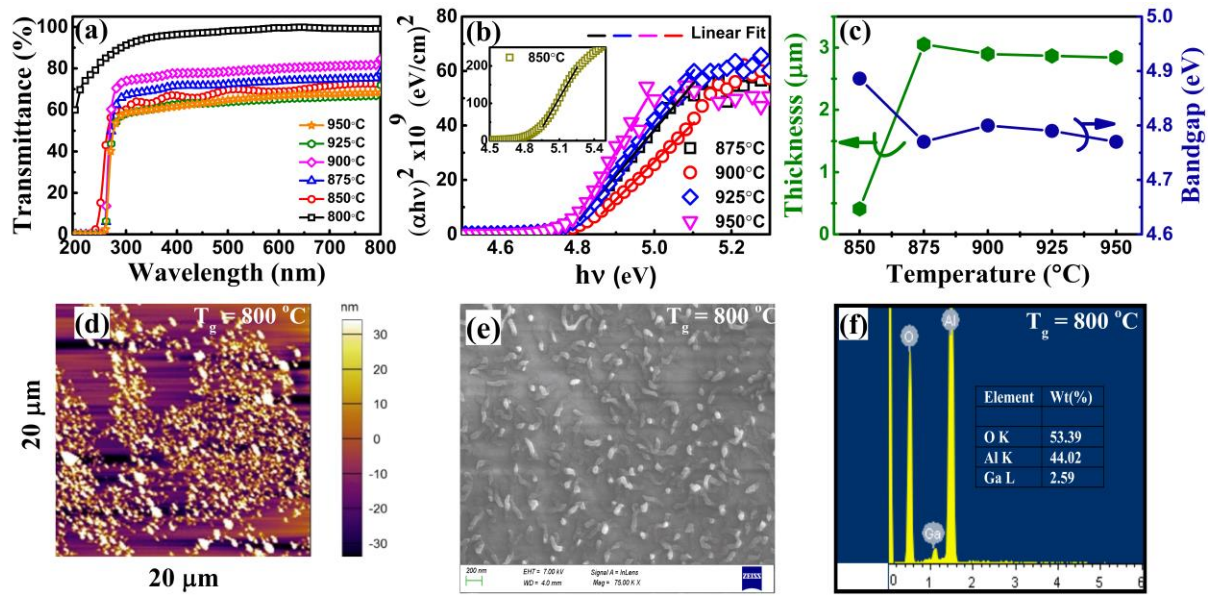


Figure 2: (a) UV Visible transmission spectroscopy, (b) Tauc plot of β -Ga₂O₃ thin films grown at different temperatures on c-plane sapphire substrate (the x- and y- axis label of inset is same as the main figure), (c) thickness (left Y axis) extracted by modelling reflectance vs wavelength data and bandgap (right Y axis) obtained from Tauc plot of β -Ga₂O₃ thin films with respect to the growth temperature (solid line is only given as a guide to eye), and top surface (d) AFM image (e) FESEM image (scale bar 200 nm) and, (f) EDS spectra for sample grown at deposition temperature of 800 °C.

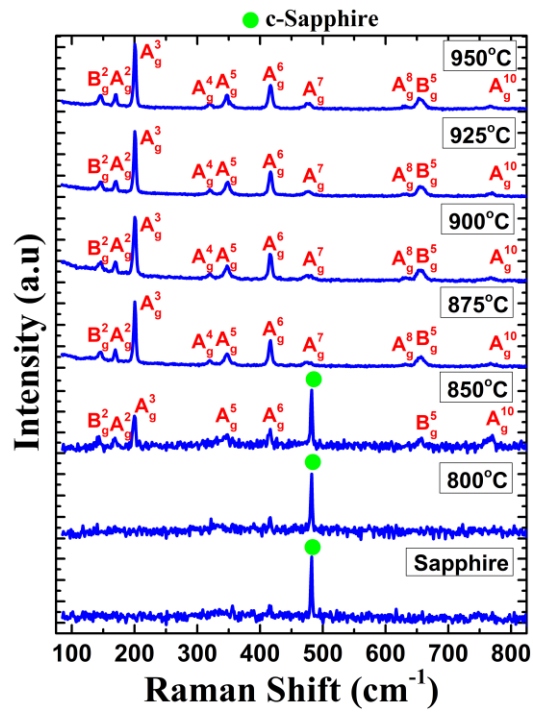


Figure 3: Experimental Raman Spectra of β -Ga₂O₃ thin films on c-plane sapphire substrates, excited by laser wavelength of $\lambda = 532$ nm, grown at different deposition temperatures.

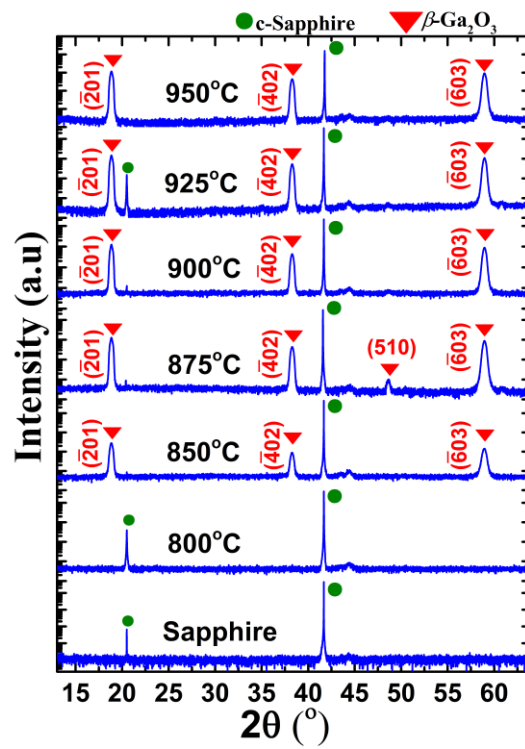


Figure 4: XRD spectra (ω - 2θ scan) of β -Ga₂O₃ thin films on c-plane sapphire substrates grown at different growth temperatures.

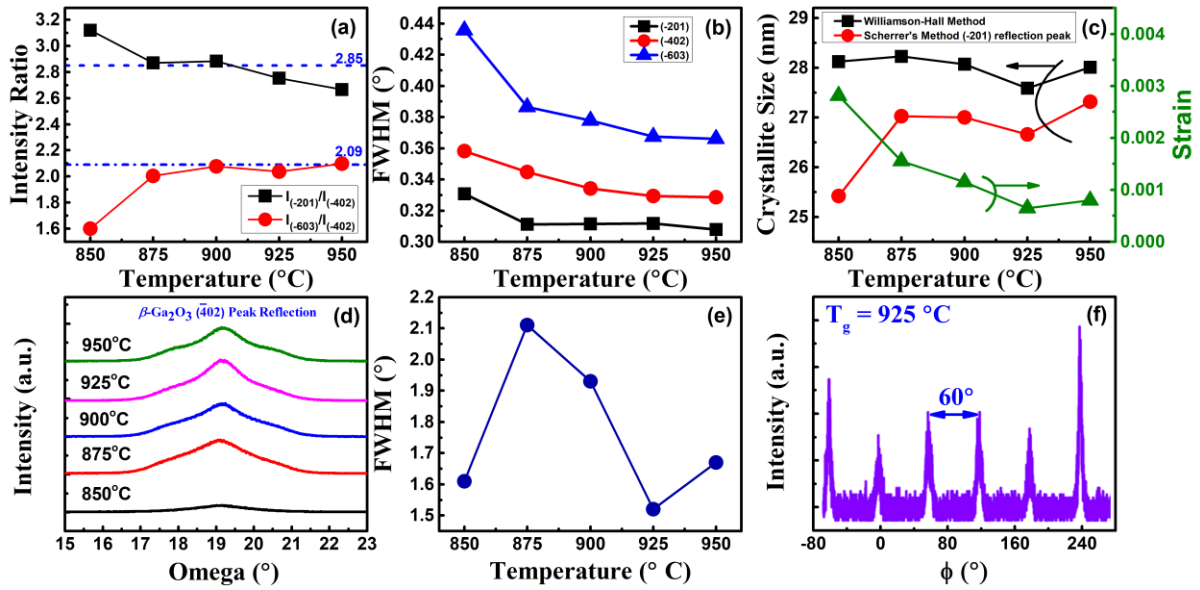


Figure 5: (a) Ratio of the intensity of (-201) and (-603) diffraction peaks to the intensity of (-402) diffraction peak (ideal intensity ratios are also marked in the figure), (b) FWHM of major peaks (-201), (-402), and (-603) from ω -2 θ scan obtained by Gaussian fit, (c) On left axis: crystallite size calculated using Scherrer's and Williamson-Hall methods, On right axis: strain calculated from W-H method at different growth temperatures, (d) XRD rocking scan of (-402) diffraction peak, (e) FWHM of (-402) diffraction peak for samples grown at different temperatures, (f) In-plane XRD ϕ scan for β -Ga₂O₃ thin film grown at substrate temperature of 925 °C (Solid lines in Fig. 5 (a), (b), (c), and (e) are for guiding purpose only).

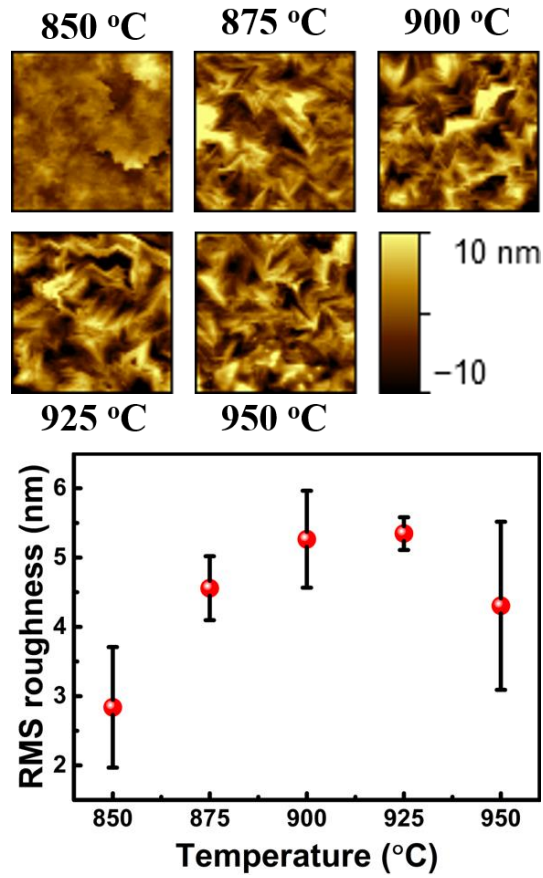


Figure 6: AFM images for the scan area of $5 \mu\text{m} \times 5 \mu\text{m}$ of β -Ga₂O₃ thin films deposited at different temperatures. Graph shows mean surface RMS roughness extracted from scan images as a function of deposition temperature.

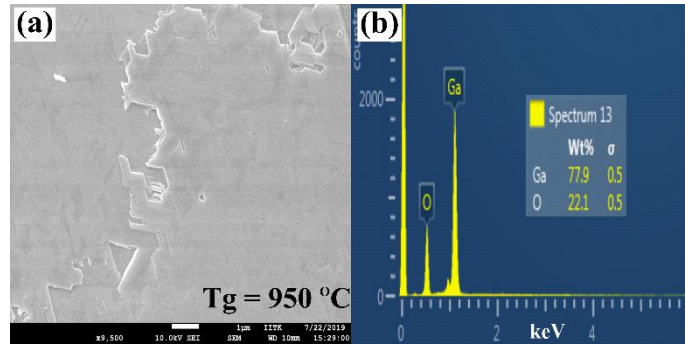


Figure 7: (a) Top view FESEM image of (-201) oriented β -Ga₂O₃ thin film (scale bar = 1 μ m), and (b) EDS spectra of β -Ga₂O₃ thin film grown at 950 °C on c-plane (0001) sapphire substrate.